Biochimica et Biophysica Acta 1798 (2010) 286–290

Contents lists available at ScienceDirect

Biochimica et Biophysica Acta

journal homepage: www.elsevier.com/locate/bbamem

Protein dynamics detected in a membrane-embedded potassium channel using two-dimensional solid-state NMR spectroscopy

Christian Ader [a], Olaf Pongs [b], Stefan Becker [c], Marc Baldus [a,*]

[a] Bijvoet Center for Biomolecular Research, Utrecht University, Padualaan 8, 3584 CH Utrecht, The Netherlands
[b] Universität Hamburg, Zentrum für Molekulare Neurobiologie, Institut für Neurale Signalverarbeitung, Falkenried 94, 20251 Hamburg, Germany
[c] Max-Planck-Institute for Biophysical Chemistry, Department of NMR-based Structural Biology, Am Fassberg 11, 37077 Göttingen, Germany

ARTICLE INFO

Article history:
Received 7 May 2009
Received in revised form 31 May 2009
Accepted 29 June 2009
Available online 10 July 2009

Keywords:
Dynamics
Ion channel
MAS
Membrane
Protein
Solid-state NMR

ABSTRACT

We report longitudinal ^{15}N relaxation rates derived from two-dimensional (^{15}N, ^{13}C) chemical shift correlation experiments obtained under magic angle spinning for the potassium channel KcsA-Kv1.3 reconstituted in multilamellar vesicles. Thus, we demonstrate that solid-state NMR can be used to probe residue-specific backbone dynamics in a membrane-embedded protein. Enhanced backbone mobility was detected for two glycine residues within the selectivity filter that are highly conserved in potassium channels and that are of core relevance to the filter structure and ion selectivity.

1. Introduction

Protein dynamics play an essential role for molecular function [1] and nuclear magnetic resonance (NMR) has become a premier method to probe molecular dynamics at atomic resolution in solution [2,3]. For more than two decades (see, e.g., refs. [4,5]), solid-state NMR (ssNMR) has provided spectroscopic means to study molecular structure and dynamics in a membrane environment where molecular size increases and protein structure is modulated by the presence of a surrounding bilayer matrix [6]. With recent advancements in the field of Magic-Angle-Spinning (MAS [7]) based ssNMR on membrane proteins (see, e.g., refs. [8–10]), the structural analysis of larger membrane-embedded proteins becomes feasible.

For example, we have shown that for the chimeric KcsA-Kv1.3 potassium channel, ligand binding and channel inactivation can be studied at atomic level [11–14]. KcsA-Kv1.3 shares essential structural and functional features with the KcsA channel first identified in the gram-positive bacterium *Streptomyces lividans* [15]. KcsA has been characterized by a variety of structural and biophysical techniques and high resolution structural information is available [16–18]. The selectivity filter which entails the channel's high K^+ selectivity and specificity [19] constitutes an essential part of the K^+ channel and is highly conserved among potassium channels. During pH-induced activation KcsA and KcsA-Kv1.3 channels rapidly inactivate. The inactivation is correlated with a conformational change of the filter from a conductive to a 'collapsed' conformation which renders potassium binding sites inaccessible and thereby blocks the passage of potassium ions.

Crystal structures initiated a series of in-silico molecular-dynamics (MD) studies [20–25] that addressed the conformational flexibility in the selectivity filter for the selective conduction of potassium ions. The dynamical dependence between filter and permeant ion was referred to as breathing motion and linked to the fundamental mechanism of ion gating [25]. MD simulations evaluating the energetics related to different ion occupancies within the selectivity filter suggested a two state conduction pathway for the permeant ion [21,26]. This is supported by electron density profiles obtained for K^+ and larger analogues like Rb^+ located in the selectivity filter of KcsA [27]. Experiment and simulation showed that filter stability depends crucially on the presence of potassium [17,23,28–30]. Mutations in the selectivity filter and within its close proximity strongly affect stability and gating properties of the potassium channel [31–36], confirming that conformational dynamics of the selectivity filter and its molecular environment play an important role for channel gating [31,32,37–47].

In principle, ssNMR provides an experimental means to directly examine ion channel dynamics in a bilayer environment and in different functional states. Compared to solution-state NMR, ssNMR provides a more direct measure for internal mobility, as no overall tumbling of the molecule has to be considered. Moreover, spectral resolution is not determined by the micellar surrounding, instead the type and nature of the lipid bilayer can be readily varied granting insight into membrane effects on protein structure and dynamics (see, e.g., [48,49], Ader et al., in preparation). For KcsA-Kv1.3, previous

* Corresponding author.
E-mail address: m.baldus@uu.nl (M. Baldus).

0005-2736/$ – see front matter © 2009 Elsevier B.V. All rights reserved.
doi:10.1016/j.bbamem.2009.06.023

dipolar ssNMR correlation spectra speak in favor of a well defined structure in a membrane setting [12]. Here, we probed ^{15}N nuclear spin relaxation times to obtain a more detailed view of KcsA-Kv1.3 backbone dynamics with particular attention to selectivity filter residues. Following pioneering work by Torchia et al. [50,51] and more recent studies [52,53] on solid-phase globular proteins, we show that two-dimensional ssNMR in combination with ^{15}N-edited relaxation filtered spectroscopy provides a promising means to probe channel backbone dynamics in lipid bilayers.

2. Material and methods

Protein expression, isotope-labeling and reconstitution in asolectin liposomes were done as previously described [14]. The sample used for this study contained approximately 150 nmol (10 mg) uniformly (^{13}C, ^{15}N) labeled KcsA-Kv1.3. The protein to lipid ratio was 1:100 (mol/mol) and the water content of the sample was about 50% (w/w). Site-specific ^{15}N nuclear longitudinal relaxation rates (R_1) were measured using two-dimensional R_1-edited (^{15}N,^{13}C) correlation experiments. The corresponding pulse sequence is shown in Fig. 1 and was adapted from previous R_1 investigations [52,53] on a microcrystalline protein by incorporation of a SPECIFIC-CP [54,55] transfer step. As a result, the ^{15}N,^{13}C heteronuclear correlation spectrum is dominated by N-Cα correlations. All spectra were obtained at about 283 K and 12.5 kHz MAS using an 800 MHz instrument (Bruker Biospin Karlsruhe). The ^{1}H–^{15}N cross polarization (CP) step employed a linear ramp (100 to 80% field strength) on the ^{1}H channel. The CP period was 0.75 ms and the ^{15}N field strength was set to 35 kHz. The 2.5 ms ^{15}N–^{13}C CP step used a linear ramp on the ^{13}C channel and a ^{15}N field strength of about 34 kHz establishing SPECIFIC [54,55] transfer. ^{1}H decoupling was obtained by SPINAL64 [56] and continuous wave (CW) with a decoupling field of 83.3 kHz. Spectra were obtained for three spin-lattice relaxation times (5, 10, and 20 s). We acquired 176–560 scans for each of the 40 increments in t_1. Maximum acquisition times in t_1 and t_2 were 4 ms and 10 ms, respectively. The total experimental time for the spectra analyzed was about 140 h. In order to minimize effects due to changes in CP-efficiencies over the course of the experiment, spectra were acquired in interleaved steps and added after the whole dataset was completed. Furthermore, we monitored CP-efficiencies in between individual two-dimensional (2D) experiments by acquiring 1D control spectra. During the course of data collection, we did not observe any sizable intensity changes in the ssNMR spectra. The average ^{15}N nuclear longitudinal relaxation rate of KcsA-Kv1.3 was measured by fitting the integrals of a series of 1D ^{1}H–^{15}N cross polarization (CP) spectra with an additional spin-lattice relaxation time before detection. For the external magnetic field of 18.8 T we obtained an average relaxation rate of 0.024 s^{-1} measured at an effective temperature of 283 K. This value compares favorably to values found for a microcrystalline protein [52,53].

3. Results and discussion

As previously shown [14], KcsA-Kv1.3 residues Thr75, Gly77, and Gly79 are essential for binding K^+ ions in the selectivity filter. These

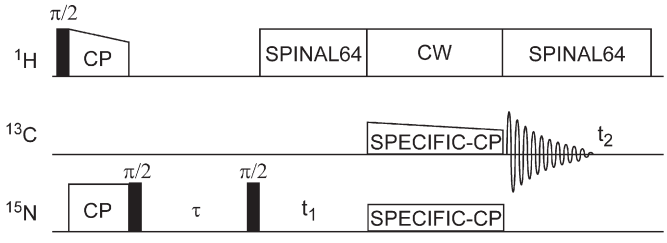

Fig. 1. Pulse sequence used to encode ^{15}N spin-lattice relaxation rates in ^{15}N–^{13}C correlation spectra. All spectra were obtained at about 283 K and 12.5 kHz MAS.

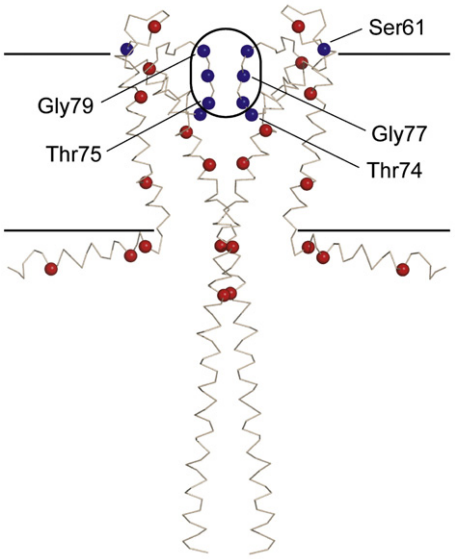

Fig. 2. Structural model for KcsA-Kv1.3 comprising residues 1–160 (only 2 subunits of the channel are shown) based on the crystal structure of full-length KcsA (PDB ID 3EFF) [18] and a full-length model based on EPR data for residues 1–24 (PDB ID 1F6G) [66]. Residues stated in the text and the following figures are labeled. Nitrogen atoms for which site-specific longitudinal relaxation rates (R_1) could be obtained are illustrated as blue spheres. Gly residues other than Gly77 and Gly79 are marked by red spheres. The selectivity filter of the potassium channel is marked by a black frame. The lipid bilayer is indicated by black lines.

residues can readily be resolved in N-Cα correlation spectra. Our spectral analysis also included Thr74, close to the inner entrance of the filter, and Ser61, located in the turret region at the extra-cellular side of the KcsA-Kv1.3 channel (Fig. 2). Together with a set of α-helical Gly residues, several residue-specific probes were hence available for spectroscopic analysis (Figs. 2, 3). Obviously, the number of residues to be investigated could be increased by conducting NCACB [57] experiments, possibly even in three spectral dimensions. For reasons of spectroscopic sensitivity, such experiments were not attempted here.

In Fig. 3, we present relaxation-edited N-Cα correlation spectra obtained for longitudinal ^{15}N delays of 5 and 20 s. Visual inspection of the spectra readily revealed a qualitative difference between residues Gly77 and Gly79, which occur at the upper, and Thr74 and Thr75, which occur at the lower part of the selectivity filter. Our data show

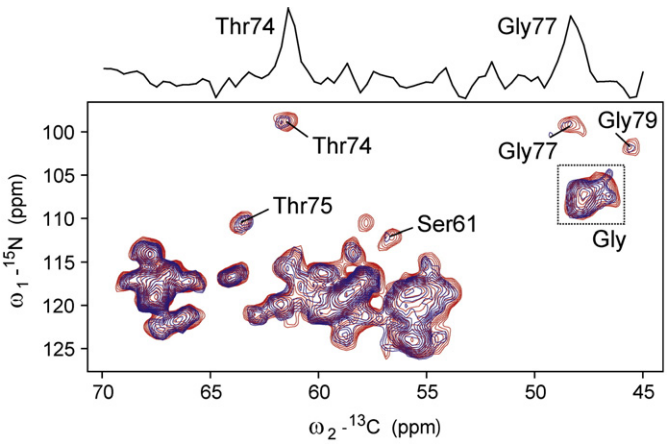

Fig. 3. Superposition of ^{15}N–^{13}C correlation spectra obtained for membrane-embedded KcsA-Kv1.3 using ^{15}N spin-lattice relaxation delays of $\tau = 5$ s (red) and $\tau = 20$ s (blue). Resonances due to residues discussed in the text are labeled. The Gly N-Cα region is marked by a dashed box. The slice on top was extracted from the spectrum employing $\tau = 5$ s at a ^{15}N chemical shift of 99 ppm in order to illustrate signal-to-noise.

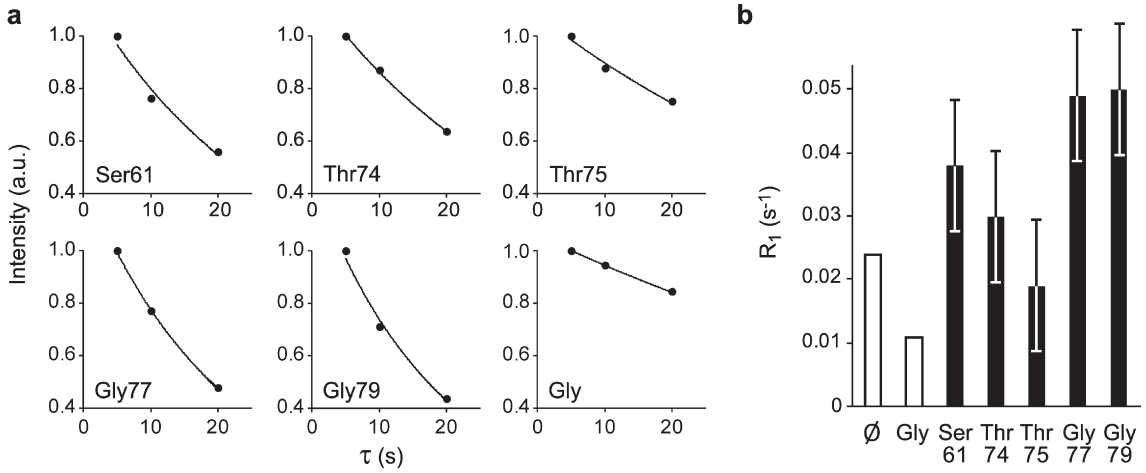

Fig. 4. (a) Decay curves measured for Ser61, Thr74, Thr75, Gly77, Gly79, and the Gly N-Cα region. Corrected intensity values obtained for three relaxation delays ($\tau = 5, 10$, and 20 s) were renormalized so that the data point for $\tau = 5$ s has an intensity value of 1. Solid curves give exponential fits to the data. (b) Bar graph summarizing the determined average (Ø) and site-specific ^{15}N spin-lattice relaxation rates.

that spin-lattice relaxation proceeds faster for Gly77 and Gly79 than for Thr74 and Thr75. In order to distinguish whether this observation originates from increased local mobility in the upper part of the selectivity filter or from larger motional freedom intrinsic for Gly residues, we included the Gly N-Cα region (dashed box in Fig. 3) in our analysis. KcsA-Kv1.3 contains thirteen glycines per subunit, mainly located in helical segments of the KcsA-Kv1.3 channel (see Fig. 2). Subsequently, we determined peak volumes for the five resolved signals and the Gly region and subtracted noise levels by integrating and subtracting corresponding noise regions of the individual spectra in order to avoid systematic overestimation of small peak volumes obtained at long relaxation delays. In order to correct for different experiment times, we normalized peak volumes by the number of acquired scans. The resulting corrected peak integrals were standardized to the respective data point obtained for the relaxation delay of 5 s and data were fitted to an exponential decay in order to determine R_1's (Fig. 4a). No correction for effects of magic angle spinning on R_1 and ^{15}N spin diffusion [52,53] was applied. Based on the signal-to-noise of our spectra, we estimate that our site-specific R_1's are associated with an error of approximately 0.01 s^{-1}.

For residues Gly77 and Gly79 we measured ^{15}N backbone R_1's of 0.049 s^{-1} and 0.050 s^{-1}, respectively (Fig. 4b). These values are significantly larger than the average value obtained for KcsA-Kv1.3. Note other signals contributing to the Gly N-Cα region are characterized by a comparatively slow relaxation rate of 0.011 s^{-1}, more than four times smaller than the relaxation rates obtained for the two Gly residues in the selectivity filter. On the other hand, we found ^{15}N backbone R_1's of residues Thr74 and Thr75 of 0.03 s^{-1} and 0.019 s^{-1}, respectively. The data suggest that increased mobility as observed for Gly77 and Gly79 is locally confined to the upper part of the selectivity filter. By contrast, Thr74 and Thr75 at the lower part of the selectivity filter have a local mobility similar to the average mobility in a channel backbone residue. In this context, it is interesting to note that mutation of Thr75 was not only found to change ion affinity but also substantially affected the thermal stability of the channel tetramer [33]. These findings suggest that this residue plays an important role for the integrity of the channel's quaternary structure in agreement with our finding that the lower part of the selectivity filter exhibits less backbone dynamics than the remaining filter segments. Finally, we determined a ^{15}N backbone R_1 of 0.038 s^{-1} for Ser61. This residue is located in the extra-cellular loop of KcsA-Kv1.3 and displays mobility above the protein's average. Nevertheless, the Ser61 value does not exceed T_1 rates observed for the Gly residues in the upper selectivity filter. The data is consistent with the idea that residues in the turret region are well structured in the resting state of the channel at pH 7.5 [12] but likely exhibit higher molecular dynamics in the context of pH-induced gating [14].

On the basis of ^{15}N backbone R_1's we have color coded in Fig. 5a the relative differences in local mobility observed for KcsA-Kv1.3 filter residues. For reference, selectivity filter residues affected by ligands which induce a distorted conductive (KTX, ref. [11,58]) or collapsed (porphyrin, ref. [14]) backbone structure are indicated. Interestingly, filter residues identified as mobile are involved in both ligand binding modes. Next, we compared our results to crystallographic B-factors obtained for KcsA crystallized in the absence and presence of an FAB antibody (Fig. 5b, c). Neither of the two data sets shows qualitative agreement to our spectroscopic analysis. This disagreement may originate from the different conditions in which the KcsA channel structures were studied including parameters like pH, temperature, ionic strength, and lipid environment. The crystal structures for example were obtained using detergent solubilized KcsA, whereas ssNMR experiments utilize proteoliposome preparations. In fact, comparison of both X-ray data sets suggests that B-factors seem to depend mainly on the environment of the channel, i.e, residing in a free crystalline state or when bound to an FAB antibody.

Previously, solution-state NMR studies of KcsA variants were conducted at pH 7.5 in SDS micelles that revealed a molecular conformation comparable to the available crystal structures and allowed to examine ^{15}N relaxation rates as a quantitative measure of structural mobility [59,60]. These data suggested increased backbone mobility for the N- and C-terminal segments of closed KcsA and excluded backbone dynamics on the ps–ns time scale for selectivity filter residues at neutral pH. However, pH-induced gating could not be followed under such conditions. Instead, solution-state NMR of KcsA in DDM and foscoline micelles was used to gain insight in pH sensing and dynamics related to activation gating [61,62]. For example, Riek et al. followed structural dynamics of residue Tyr78 in the selectivity filter as a function of pH based on $^3J(^1HN,^1H\alpha)$ scalar couplings [61]. This data revealed millisecond timescale motions in the filter that were attributed to exchange between low and high K^+ affinity states.

On the other hand, we previously observed significantly larger structural changes after inactivation in lipid bilayers [14] compared to solution-state NMR studies. It suggests that protein dynamics are significantly different in a micellar versus a lipid bilayer environment. This is consistent with the idea that composition and mechanical status of the lipid bilayer have a profound influence on K^+ channel gating and stability, underlining the utility of ssNMR-based dynamic studies in a native or native-like membrane setting. Here, we showed that ^{15}N R_1's are accessible for KcsA-Kv1.3 in a membrane setting revealing increased backbone dynamics in the upper selectivity filter

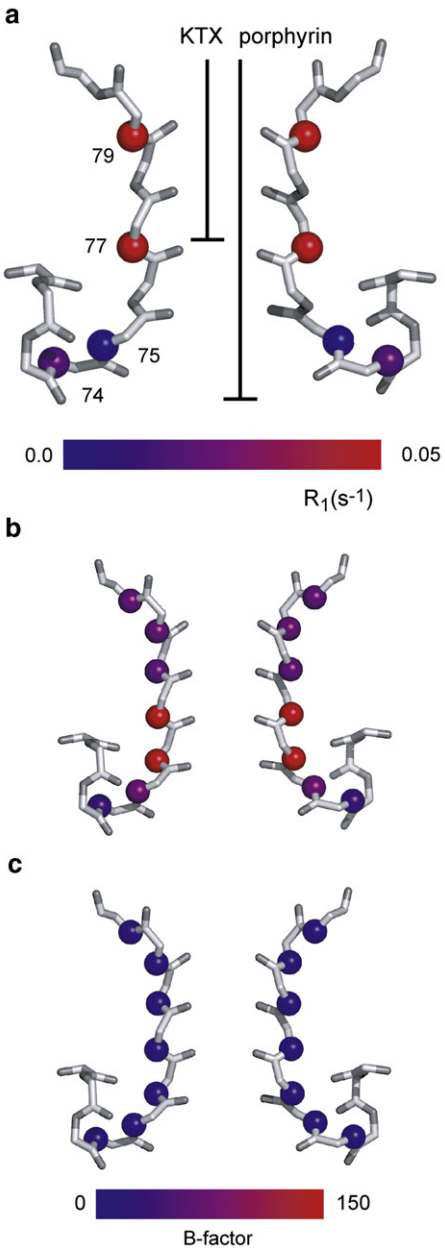

Fig. 5. (a) Selectivity filter of KcsA (PDB ID 1K4C) [17]. Backbone nitrogens for which R_1's were determined are depicted as spheres. R_1's are indicated by a color gradient from blue ($R_1 = 0\ s^{-1}$) to red ($R_1 = 0.05\ s^{-1}$). Bars indicate the residues affected by KTX and porphyrin binding, respectively. B-factors reported for backbone nitrogens of the selectivity filter and the two neighboring residues for KcsA crystal structures obtained in the absence (b, PDB ID 1BL8) [16] and presence (c, PDB ID 1K4C) [17] of FAB antibodies. B-factors are indicated by a color gradient from blue ($B = 0$) to red ($B = 150$).

of the closed channel at neutral pH. This approach may be used in the future to follow filter dynamics as a function of parameters such as pH or ion concentration controlling potassium channel function.

4. Conclusions

We have determined ^{15}N longitudinal relaxation rates for individual residues of KcsA-Kv1.3 in lipid bilayers. The experiments allow for a qualitative description of local backbone dynamics in the selectivity filter in reference to other segments of a membrane-embedded potassium channel. Site-specific R_1's ranged from 0.019 s^{-1} to 0.050 s^{-1} at 18.8 T and the average protein backbone relaxation can be described by an overall rate of 0.024 s^{-1}. In absolute numbers, the values compare favorably to data obtained on a crystalline protein at different magnetic fields. Our experiments confirm earlier conclusions based on dipolar ssNMR correlation spectroscopy [12] that KcsA-Kv1.3 resides in a well defined structure in a membrane setting. We observe a locally increased mobility for Gly77 and Gly79 in the upper part of the KcsA-Kv1.3 selectivity filter, while the Thr74 and Thr75 residues in the lower part display local dynamics similar to the average protein backbone. The two glycine residues are highly conserved in the pore of K^+ channels and their conformational dynamics are of crucial importance to the filter structure and ion selectivity (see, e.g., refs. [34,35]). Here, we found that these residues are also characterized by distinctly high backbone mobility. We propose that this mobility is an essential property of the filter to dynamically respond to the binding and unbinding of ions while they pass along the K^+ binding sites in the filter during ion permeation. Furthermore, conformational backbone plasticity of the selectivity filter may be critical for the gating transitions of the K^+ channel involving conductive and 'collapsed' filter conformations or the binding of ligands to the K^+ channel pore. The results underline that T_1 relaxation rates provide a powerful means to follow site-specific dynamics in larger membrane-embedded proteins by solid-state NMR. To further dissect dynamical details associated with K^+ channel function, site-resolved measurement of ^{15}N backbone dynamics may in the future be assisted by measurements of transversal protein relaxation rates [63] or by a more detailed analysis of ssNMR chemical shifts and cross-peak amplitudes as recently demonstrated for other membrane proteins [64,65].

Acknowledgements

This work was funded in part by NWO and the DFG. C.A. is supported by a Kekule fellowship of the Stiftung Stipendien-Fonds of the Verband der Chemischen Industrie, Germany.

References

[1] R.G. Smock, L.M. Gierasch, Sending signals dynamically, Science 324 (2009) 198–203.
[2] D.D. Boehr, D. McElheny, H.J. Dyson, P.E. Wright, The dynamic energy landscape of dihydrofolate reductase catalysis, Science 313 (2006) 1638–1642.
[3] A. Mittermaier, L.E. Kay, New tools provide new insights in NMR studies of protein dynamics, Science 312 (2006) 224–228.
[4] J. Seelig, Deuterium magnetic-resonance — theory and application to lipid-membranes, Q. Rev. Biophys. 10 (1977) 353–418.
[5] J. Herzfeld, A. Roufosse, R.A. Haberkorn, R.G. Griffin, M.J. Glimcher, Magic angle sample spinning in inhomogeneously broadened biological-systems, Philos. Trans. R. Soc. Lond., Ser. B Biol. Sci. 289 (1980) 459–469.
[6] R.B. Gennis, Biomembranes: Molecular Structure and Function, Springer, New York, 1989.
[7] E.R. Andrew, A. Bradbury, R.G. Eades, Nuclear magnetic resonance spectra from a crystal rotated at high speed, Nature 182 (1958) 1659.
[8] M. Hong, Structure, topology, and dynamics of membrane peptides and proteins from solid-state NMR spectroscopy, J. Phys. Chem. B 111 (2007) 10340–10351.
[9] N.J. Traaseth, K.N. Ha, R. Verardi, L. Shi, J.J. Buffy, L.R. Masterson, G. Veglia, Structural and dynamic basis of phospholamban and sarcolipin inhibition of Ca^{2+}-aTPase, Biochemistry 47 (2008) 3–13.
[10] U.H.N. Dürr, L. Waskell, A. Ramamoorthy, The cytochromes P450 and b5 and their reductases—promising targets for structural studies by advanced solid-state NMR spectroscopy, Biochim. Biophys. Acta Biomembr. 1768 (2007) 3235–3259.
[11] A. Lange, K. Giller, S. Hornig, M.-F. Martin-Eauclaire, O. Pongs, S. Becker, M. Baldus, Toxin-induced conformational changes in a potassium channel revealed by solid-state NMR, Nature 440 (2006) 959–962.
[12] R. Schneider, C. Ader, A. Lange, K. Giller, S. Hornig, O. Pongs, S. Becker, M. Baldus, Solid-state NMR spectroscopy applied to a chimeric potassium channel in lipid bilayers, J. Am. Chem. Soc. 130 (2008) 7427–7435.
[13] C. Ader, R. Schneider, K. Seidel, M. Etzkorn, S. Becker, M. Baldus, Structural rearrangements of membrane proteins probed by water-edited solid-state NMR spectroscopy, J. Am. Chem. Soc. 131 (2009) 170–176.
[14] C. Ader, R. Schneider, S. Hornig, P. Velisetty, E.M. Wilson, A. Lange, K. Giller, I. Ohmert, M.-F. Martin-Eauclaire, D. Trauner, S. Becker, O. Pongs, M. Baldus, A structural link between inactivation and block of a K^+ channel, Nat. Struct. Mol. Biol. 15 (2008) 605–612.
[15] H. Schrempf, O. Schmidt, R. Kummerlen, S. Hinnah, D. Muller, M. Betzler, T. Steinkamp, R. Wagner, A prokaryotic potassium-ion channel with 2 predicted transmembrane segments from *Streptomyces-lividans*, EMBO J. 14 (1995) 5170–5178.
[16] D.A. Doyle, J. Morais-Cabral, R.A. Pfuetzner, A. Kuo, J.M. Gulbis, S.L. Cohen, B.T. Chait,

R. MacKinnon, The structure of the potassium channel: molecular basis of K^+ conduction and selectivity, Science 280 (1998) 69–77.
[17] Y. Zhou, J.H. Morais-Cabral, A. Kaufman, R. MacKinnon, Chemistry of ion coordination and hydration revealed by a K^+ channel-Fab complex at 2.0 Å resolution, Nature 414 (2001) 43–48.
[18] S. Uysal, V. Vasquez, V. Tereshko, K. Esaki, F.A. Fellouse, S.S. Sidhu, S. Koide, E. Perozo, A. Kossiakoff, Crystal structure of full-length KcsA in its closed conformation, Proc. Natl. Acad. Sci. U. S. A. 106 (2009) 6644–6649.
[19] R. MacKinnon, Potassium channels and the atomic basis of selective ion conduction (Nobel lecture), Angew. Chem., Int. Ed. 43 (2004) 4265–4277.
[20] T.W. Allen, S. Kuyucak, S.H. Chung, Molecular dynamics study of the KcsA potassium channel, Biophys. J. 77 (1999) 2502–2516.
[21] J. Aqvist, V. Luzhkov, Ion permeation mechanism of the potassium channel, Nature 404 (2000) 881–884.
[22] S. Bernèche, B. Roux, Molecular dynamics of the KcsA K^+ channel in a bilayer membrane, Biophys. J. 78 (2000) 2900–2917.
[23] L. Guidoni, V. Torre, P. Carloni, Potassium and sodium binding to the outer mouth of the K^+ channel, Biochemistry 38 (1999) 8599–8604.
[24] I.H. Shrivastava, C.E. Capener, L.R. Forrest, M.S.P. Sansom, Structure and dynamics of K channel pore-lining helices: a comparative simulation study, Biophys. J. 78 (2000) 79–92.
[25] I.H. Shrivastava, M.S.P. Sansom, Simulations of ion permeation through a potassium channel: molecular dynamics of KcsA in a phospholipid bilayer, Biophys. J. 78 (2000) 557–570.
[26] S. Bernèche, B. Roux, Energetics of ion conduction through the K^+ channel, Nature 414 (2001) 73–77.
[27] J.H. Morais-Cabral, Y. Zhou, R. MacKinnon, Energetic optimization of ion conduction rate by the K^+ selectivity filter, Nature 414 (2001) 37–42.
[28] C. Domene, M.S.P. Sansom, Potassium channel, ions, and water: simulation studies based on the high resolution X-ray structure of KcsA, Biophys. J. 85 (2003) 2787–2800.
[29] S.W. Lockless, M. Zhou, R. MacKinnon, Structural and thermodynamic properties of selective ion binding in a K^+ channel, PLoS Biol. 5 (2007) e121.
[30] Y. Zhou, R. MacKinnon, The occupancy of ions in the K^+ selectivity filter: charge balance and coupling of ion binding to a protein conformational change underlie high conduction rates, J. Mol. Biol. 333 (2003) 965–975.
[31] J.F. Cordero-Morales, L.G. Cuello, Y. Zhao, V. Jogini, D.M. Cortes, B. Roux, E. Perozo, Molecular determinants of gating at the potassium-channel selectivity filter, Nat. Struct. Mol. Biol. 13 (2006) 311–318.
[32] J.F. Cordero-Morales, V. Jogini, A. Lewis, V. Vasquez, D.M. Cortes, B. Roux, E. Perozo, Molecular driving forces determining potassium channel slow inactivation, Nat. Struct. Mol. Biol. 14 (2007) 1062–1069.
[33] M.N. Krishnan, P. Trombley, E.G. Moczydlowski, Thermal stability of the K^+ channel tetramer: cation interactions and the conserved threonine residue at the innermost site (S4) of the KcsA selectivity filter, Biochemistry 47 (2008) 5354–5367.
[34] F.I. Valiyaveetil, M. Leonetti, T.W. Muir, R. MacKinnon, Ion selectivity in a semi-synthetic K^+ channel locked in the conductive conformation, Science 314 (2006) 1004–1007.
[35] F.I. Valiyaveetil, M. Sekedat, R. MacKinnon, T.W. Muir, Glycine as a D-amino acid surrogate in the K^+-selectivity filter, Proc. Natl. Acad. Sci. U. S. A. 101 (2004) 17045–17049.
[36] M. Zhou, R. MacKinnon, A mutant KcsA K^+ channel with altered conduction properties and selectivity filter ion distribution, J. Mol. Biol. 338 (2004) 839–846.
[37] S. Bernèche, B. Roux, A gate in the selectivity filter of potassium channels, Structure 13 (2005) 591–600.
[38] R. Blunck, J.F. Cordero-Morales, L.G. Cuello, E. Perozo, F. Bezanilla, Detection of the opening of the bundle crossing in KcsA with fluorescence lifetime spectroscopy reveals the existence of two gates for ion conduction, J. Gen. Physiol. 128 (2006) 569–581.
[39] A.M.J. VanDongen, K channel gating by an affinity-switching selectivity filter, Proc. Natl. Acad. Sci. U. S. A. 101 (2004) 3248–3252.
[40] S. Chakrapani, J.F. Cordero-Morales, E. Perozo, A quantitative description of KcsA gating I: Macroscopic currents, J. Gen. Physiol. 130 (2007) 465–478.
[41] S. Chakrapani, J.F. Cordero-Morales, E. Perozo, A quantitative description of KcsA gating II: Single-channel currents, J. Gen. Physiol. 130 (2007) 479–496.
[42] L. Gao, X. Mi, V. Paajanen, K. Wang, Z. Fan, From the cover: activation-coupled inactivation in the bacterial potassium channel KcsA, Proc. Natl. Acad. Sci. U. S. A. 102 (2005) 17630–17635.
[43] L. Kiss, S.J. Korn, Modulation of C-type inactivation by K^+ at the potassium channel selectivity filter, Biophys. J. 74 (1998) 1840–1849.
[44] H.T. Kurata, D. Fedida, A structural interpretation of voltage-gated potassium channel inactivation, Prog. Biophys. Mol. Biol. 92 (2006) 185–208.
[45] Y. Liu, M.E. Jurman, G. Yellen, Dynamic rearrangement of the outer mouth of a K^+ channel during gating, Neuron 16 (1996) 859–867.
[46] E.M. Ogielska, R.W. Aldrich, Functional consequences of a decreased potassium affinity in a potassium channel pore. ion interactions and C-type inactivation, J. Gen. Physiol. 113 (1999) 347–358.
[47] J. Zheng, F.J. Sigworth, Selectivity changes during activation of mutant shaker potassium channels, J. Gen. Physiol. 110 (1997) 101–117.
[48] R. Mani, S.D. Cady, M. Tang, A.J. Waring, R.I. Lehrer, M. Hong, Membrane-dependent oligomeric structure and pore formation of a β-hairpin antimicrobial peptide in lipid bilayers from solid-state NMR, Proc. Natl. Acad. Sci. U. S. A. 103 (2006) 16242–16247.
[49] J. Xu, U.H.N. Dürr, S.-C. Im, Z. Gan, L. Waskell, A. Ramamoorthy, Bicelle-enabled structural studies on a membrane-associated cytochrome *b*5 by solid-state MAS NMR spectroscopy, Angew. Chem., Int. Ed. 47 (2008) 7864–7867.
[50] D.A. Torchia, Solid-state NMR-studies of protein internal dynamics, Annu. Rev. Biophys. Bioeng. 13 (1984) 125–144.
[51] H.B.R. Cole, D.A. Torchia, An NMR-study of the backbone dynamics of staphylococcal nuclease in the crystalline state, Chem. Phys. 158 (1991) 271–281.
[52] N. Giraud, A. Böckmann, A. Lesage, F. Penin, M. Blackledge, L. Emsley, Site-specific backbone dynamics from a crystalline protein by solid-state NMR spectroscopy, J. Am. Chem. Soc. 126 (2004) 11422–11423.
[53] N. Giraud, M. Blackledge, M. Goldman, A. Böckmann, A. Lesage, F. Penin, L. Emsley, Quantitative analysis of backbone dynamics in a crystalline protein from nitrogen-15 spin-lattice relaxation, J. Am. Chem. Soc. 127 (2005) 18190–18201.
[54] M. Baldus, A.T. Petkova, J. Herzfeld, R.G. Griffin, Cross polarization in the tilted frame: assignment and spectral simplification in heteronuclear spin systems, Mol. Phys. 95 (1998) 1197–1207.
[55] A.T. Petkova, M. Baldus, M. Belenky, M. Hong, R.G. Griffin, J. Herzfeld, Backbone and side chain assignment strategies for multiply labeled membrane peptides and proteins in the solid state, J. Magn. Reson. 160 (2003) 1–12.
[56] B.M. Fung, A.K. Khitrin, K. Ermolaev, An improved broadband decoupling sequence for liquid crystals and solids, J. Magn. Reson. 142 (2000) 97–101.
[57] M. Baldus, Correlation experiments for assignment and structure elucidation of immobilized polypeptides under magic angle spinning, Prog. Nucl. Magn. Reson. Spectrosc. 41 (2002) 1–47.
[58] U. Zachariae, R. Schneider, P. Velisetty, A. Lange, D. Seeliger, S.J. Wacker, Y. Karimi-Nejad, G. Vriend, S. Becker, O. Pongs, M. Baldus, B.L. de Groot, The molecular mechanism of toxin-induced conformational changes in a potassium channel: relation to C-type inactivation, Structure 16 (2008) 747–754.
[59] J.H. Chill, J.M. Louis, J.L. Baber, A. Bax, Measurement of ^{15}N relaxation in the detergent-solubilized tetrameric KcsA potassium channel. J. Biomol. NMR 36 (2007) 123–136.
[60] J.H. Chill, J.M. Louis, C. Miller, A. Bax, NMR study of the tetrameric KcsA potassium channel in detergent micelles, Protein Sci. 15 (2006) 684–698.
[61] K.A. Baker, C. Tzitzilonis, W. Kwiatkowski, S. Choe, R. Riek, Conformational dynamics of the KcsA potassium channel governs gating properties, Nat. Struct. Mol. Biol. 14 (2007) 1089–1095.
[62] K. Takeuchi, H. Takahashi, S. Kawano, I. Shimada, Identification and characterization of the slowly exchanging pH-dependent conformational rearrangement in KcsA, J. Biol. Chem. 282 (2007) 15179–15186.
[63] S.D. Cady, M. Hong, Amantadine-induced conformational and dynamical changes of the influenza M2 transmembrane proton channel, Proc. Natl. Acad. Sci. U. S. A. 105 (2008) 1483–1488.
[64] K. Seidel, O.C. Andronesi, J. Krebs, C. Griesinger, H.S. Young, S. Becker, M. Baldus, Structural characterization of Ca^{2+}-ATPase-bound phospholamban in lipid bilayers by solid-state nuclear magnetic resonance (NMR) spectroscopy, Biochemistry 47 (2008) 4369–4376.
[65] M. Etzkorn, H. Kneuper, P. Dunnwald, V. Vijayan, J. Kramer, C. Griesinger, S. Becker, G. Unden, M. Baldus, Plasticity of the PAS domain and a potential role for signal transduction in the histidine kinase DcuS, Nat. Struct. Mol. Biol. 15 (2008) 1031–1039.
[66] D.M. Cortes, L.G. Cuello, E. Perozo, Molecular architecture of full-length KcsA: role of cytoplasmic domains in ion permeation and activation gating, J. Gen. Physiol. 117 (2001) 165–180.